



Numerical analysis of water-alternating-CO₂ flooding for CO₂-EOR and storage projects in residual oil zones

Boyu Liu¹ · Jun Yao¹ · Tunan Sun¹

Received: 5 March 2023 / Revised: 6 June 2023 / Accepted: 10 August 2023
© The Author(s) 2023

Abstract

Residual oil zones (ROZs) have high residual oil saturation, which can be produced using CO₂ miscible flooding. At the same time, these zones are good candidates for CO₂ sequestration. To evaluate the coupled CO₂-EOR and storage performance in ROZs for Water-Alternating-CO₂ (WAG) flooding, a multi-compositional CO₂ miscible model with molecular diffusion was developed. The effects of formation parameters (porosity, permeability, temperature), operation parameters (bottom hole pressure, WAG ratio, pore volume of injected water), and diffusion coefficient on the coupled CO₂-EOR and storage were investigated. Five points from the CO₂ sequestration curve and the oil recovery factor curve were selected to help better analyze coupled CO₂-EOR and storage. The results demonstrate that enhanced performance is observed when formation permeability is higher and a larger volume of water is injected. On the other hand, the performance diminishes with increasing porosity, molecular diffusion of gas, and the WAG ratio. When the temperature is around 100 °C, coupled CO₂-EOR and storage performance is the worst. To achieve optimal miscible flooding, it is recommended to maintain the bottom hole pressure (BHP) of the injection well above 1.2 minimum miscibility pressure (MMP), while ensuring that the BHP of the production well remains sufficiently high. Furthermore, the tapered WAG flooding strategy proves to be profitable for enhanced oil recovery, as compared to a WAG ratio of 0.5:1, although it may not be as effective for CO₂ sequestration.

Keywords Residual oil zone · WAG injection · Carbon sequestration · Enhanced oil recovery · Injection strategies

1 Introduction

CO₂ is one of the main gases causing the greenhouse effect. With the increased amount of resources such as oil and coal consumed, the global warming problem gets worse (Liu et al. 2018). To solve the sharp increase in carbon dioxide emissions, the technology of carbon capture, utilization, and storage (CCUS) has attracted much attention in the energy industry (Jiang et al. 2020).

Under reservoir conditions, CO₂ normally exists as a supercritical fluid, which has been widely known as a favorable and promising EOR agent for decades. Miscible flooding is more effective than immiscible flooding due to the disappearance of surface tension and capillary pressure. Miscible flooding between the injected supercritical CO₂ and oil

can be achieved at pressures above the MMP (Gong and Gu 2015). Hence, the displacement pressure is supposed to be higher than MMP to ensure the miscible flooding is maintained during the whole flooding process. Many studies have shown a significant improvement in oil recovery by CO₂ miscible flooding (Brock and Bryan 1989; Farajzadeh et al. 2010; Rui et al. 2017). Recently, research on CO₂ flooding has grown because CO₂ flooding can enhance oil recovery and store a considerable amount of CO₂ underground. Thus, appropriate implementation of CO₂-EOR offers two advantages: (1) environmental benefits from storing injected CO₂ and (2) economic benefits from enhanced oil recovery.

Residual oil zones (ROZs) are portions of an oil reservoir, or even whole reservoirs, in which the oil saturations are near residual levels. These zones exhibit characteristics similar to those of a reservoir after waterflooding. ROZs are widely distributed within the Permian Basin of West Texas. Koperna et al. (2006) estimated the recoverable oil volume from ROZs in the San Andres and Canyon Reef formations of the Permian Basin to be approximately 12 billion barrels. Conventional methods, such as water flooding, are

✉ Jun Yao
junyaoup@gmail.com

¹ Research Center of Multiphase Flow in Porous Media, China University of Petroleum (East China), Qingdao 266000, China

insufficient for the production of oil from ROZs; instead, enhanced oil recovery (EOR) techniques such as CO₂-EOR becomes imperative, which incidentally sequesters CO₂. As noted by Al Eidan et al. (2015), ROZs are regarded as the most favorable reservoir sections for CO₂ storage. Consequently, the significance of CO₂ sequestration in CO₂-EOR projects is of paramount importance. Notably, ongoing

$$\frac{\partial}{\partial t} \left(\phi \sum_{\ell=1}^{N_p} \rho_{\ell} S_{\ell} w_{i\ell} \right) + \nabla \cdot \left(\sum_{\ell=1}^{N_p} \rho_{\ell} w_{i\ell} v_{\ell} - \phi \rho_{\ell} S_{\ell} D_{i\ell} \nabla w_{i\ell} \right) - r_i = 0 \quad i = 1, \dots, N_c \quad (1)$$

commercial-scale WAG injections of CO₂ into ROZs are being carried out in eight San Andres oil fields within the Permian Basin, as reported by Ren and Duncan (2019a). However, research on the coupled CO₂-EOR and storage in ROZs remains insufficient.

Several studies have investigated the optimization of CO₂-EOR storage in different types of oil reservoirs with different operation parameters. Ghaderi et al. (2012) analyzed the effect of development patterns and WAG parameters on oil recovery, CO₂ sequestration, and NPV in tight oil formations. Karimaie et al. (2017) investigated CO₂-EOR performance in high permeability layers under various flooding scenarios, such as continuous gas injection, constant water-alternating-gas injection, and tapered WAG injection. Song et al. (2014) used the orthogonal experimental design method to optimize the reservoir and operation parameters for enhanced oil recovery and CO₂ sequestration in high-water-cut oil reservoirs. Ren and Duncan (2019b) evaluated the effects of injection strategies and reservoir heterogeneities on the performance of CO₂ sequestration based on the San Andre residual oil zones. Ettehadtavakkol et al. (2014) analyzed the coupled CO₂-EOR and storage, considering reservoir properties, design parameters, and economic parameters. However, coupled CO₂-EOR and storage performance in residual oil zones still needs to be investigated. This study considers molecular diffusion and analyzes the effects of formation parameters, operation parameters, and diffusion coefficients on coupled CO₂-EOR and storage.

In this study, a multi-compositional CO₂ miscible model with molecular diffusion was developed. The effects of formation parameters (porosity, permeability, temperature), operation parameters (bottom hole pressure, WAG ratio), and diffusion coefficient on coupled CO₂-EOR and storage were analyzed. The optimum parameters under which the highest oil recovery and highest CO₂ sequestration can be achieved were investigated.

2 Methodology and model setup

2.1 Governing equations

The mass conservation equation considering molecular diffusion for each chemical component i in the oil, gas, and water phases can be presented as:

where, t is the time; ϕ is the porosity; ρ is the density; S is phase saturation; $w_{i\ell}$ is mass fraction of component i in phase ℓ ; v is Darcy's velocity; $D_{i\ell}$ is the molecular diffusion coefficient of component i in phase ℓ ; r is the injection or production mass rate; the subscripts ℓ denote oil, gas or water phase; the subscript i refers to chemical component.

The Darcy's velocity v_{ℓ} is formulated by Darcy's law.

$$v_{\ell} = -\frac{Kk_{r\ell}}{\mu_{\ell}} (\nabla P_{\ell} - \rho_{\ell} g) \quad (2)$$

where K is absolute permeability, $k_{r\ell}$ is relative permeability of phase ℓ . P_{ℓ} is phase pressure. μ_{ℓ} is phase viscosity. ρ_{ℓ} is phase density.

The mass rate r_i can be expressed as:

$$r_i = \sum_{\ell=1}^{N_p} \rho_{\ell} w_{i\ell} WI_{\ell} (p_{\text{well}}^{\ell} - p_{\text{block}}^{\ell}) \quad (3)$$

where p_{well} is wellbore pressure, p_{block} is pressure existing within block and WI is well index.

The two-phase relative permeability curves of water–oil and liquid–gas are fitted given the relative permeability tables. The three-phase relative permeability curve is generated using Stone's Model II (Stone 1970).

$$k_{ro} = (k_{rog} + k_{rg})(k_{row} + k_{rw}) - (k_{rw} + k_{rg}) \quad (4)$$

The mass exchange between the oil and gas phases is modeled by the thermodynamic equilibrium conditions, which is defined by the equality of fugacity of all components.

$$f_g^i = f_o^i \quad (5)$$

where, f_o^i is the fugacity of component i in oil phase; f_g^i is the fugacity of component i in gas phase; the Peng-Robinson EOS equations (Peng and Robinson 1976) are used to do

two-phase flash calculation, and the calculation is solved using QNMs (Quasi-Newton Methods).

The equation system is closed by the sum of saturations and concentrations.

$$S_o + S_g + S_w = 1 \tag{6}$$

$$\sum_i c_o^i = 1 \quad \sum_i c_g^i = 1 \tag{7}$$

2.2 Model setup

A three-dimensional reservoir model is built in CMG-GEM to investigate: (1) the WAG flooding performance to enhance the oil recovery; and (2) the amount of CO₂ sequestered in the reservoir. The reservoir model is 225 m, 225 m, and 18 m in the *x*, *y*, and *z* dimensions,

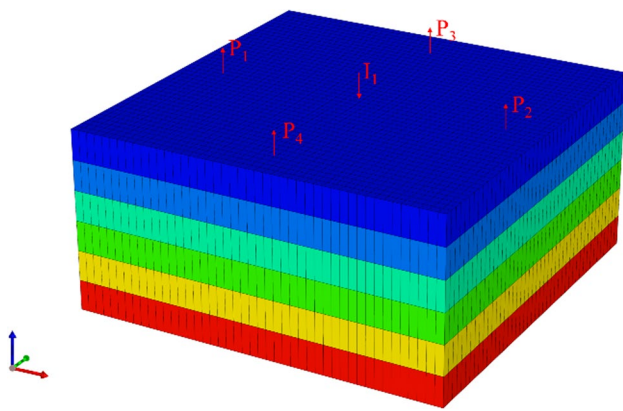


Fig. 1 Three-dimensional reservoir model with well-spacing pattern

Table 1 Basic simulation parameters

Parameter	Value	Parameter	Value
Reservoir depth (m)	2500	Permeability (mD)	20
Net pay (m)	18	Temperature (°C)	100
Porosity	0.12	Initial pressure (MPa)	23.4
Oil diffusion coefficient (cm ² /s)	1 × 10 ⁻⁶	Oil viscosity (cP)	9.27
Gas diffusion coefficient (cm ² /s)	0.01	Oil density (kg/m ³)	729
MMP (MPa)	18		

respectively. A five-spot pattern is used, with a well spacing (the distance between producers) of 220 m, as shown in Fig. 1. All six layers of the formation are perforated. The initial oil saturation, connate water saturation, and residual oil saturation for oil–water system are 0.793, 0.207, and 0.25, respectively. The connate gas saturation and maximum gas saturation for gas–liquid system are 0 and 0.422, respectively. The relative permeability curves are shown in Fig. 2. Other basic simulation parameters are summarized in Table 1.

2.3 Minimum miscible pressure (MMP) determination

The minimum miscible pressure (MMP) was calculated in CMG-WinProp. The components of reservoir oil were lumped into seven pseudo-components, and the parameters of the Peng-Robinson equation of state were fitted based on the experiment data from the constant composition expansion (CCE) test, the differential liberation (DL) test, and the swelling test (ST). The regression procedure by Agarwal et al. (1987) was used to improve

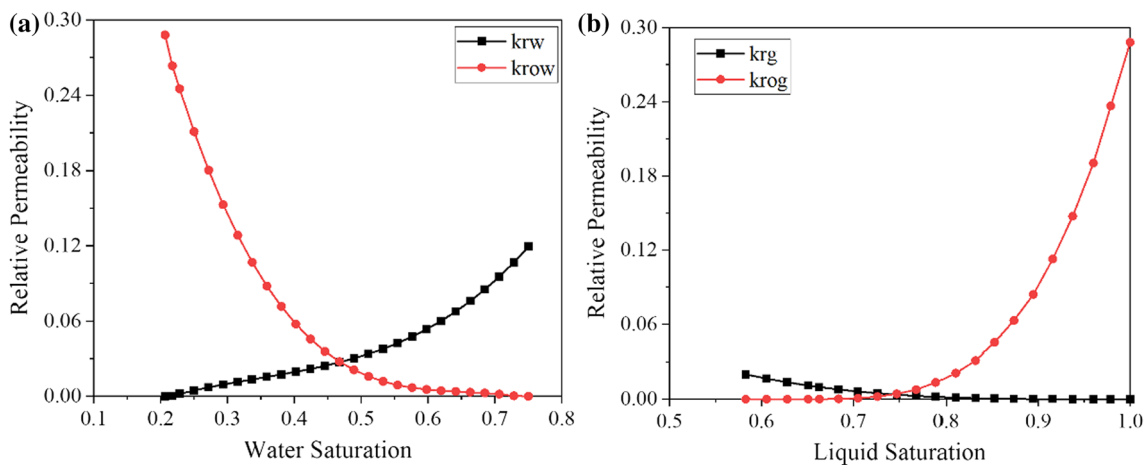


Fig. 2 Relative permeability curves of a The water–oil system and b The gas–liquid system for the base reservoir model

Table 2 The pseudo-component description of crude oil

Component	Mole fraction	Molecular weight (g/gmol)	T_c (K)	P_c (bar)
H ₂ S–CO ₂	0.0128	44.01	304.2	72.8
N ₂ –CH ₄	0.1275	16.21	189.6	45.2
C ₂ H–NC ₄	0.2069	44.14	368.8	42.2
IC ₅ –C ₇	0.1712	98.59	380	27
IC ₈ –C ₁₂	0.1766	93.92	490	25
IC ₁₃ –C ₂₀	0.1265	130	580	24
IC ₂₁ –C ₃₀	0.1785	353.9	690	19.4

the regression efficiency. The fitted pseudo-component description of crude oil is shown in Table 2. In this case, the traditional Cell-to-Cell simulation method, which uses a vaporizing drive mechanism, was utilized to calculate MMP. The MMP calculated is 18 MPa in this case. The miscible flooding is achieved at pressures above MMP, as described by the interfacial tension decreasing to zero in the CMG-GEM model.

3 Results and discussion

This section initiates with the simulation of a comprehensive production process, consisting of depletion-drive, water flooding, and WAG flooding, aimed at emulating the conditions prevalent in the residual oil zone. Following this, an extensive comparison is carried out to assess the performance of water flooding, continuous CO₂ flooding, and CO₂ WAG flooding. Finally, a sensitivity analysis is performed to examine the impact of formation parameters, operation parameters, and diffusion coefficients.

3.1 Base case

In this section, a complete production process is described, and three flooding methods are compared. The reservoir is under depletion-driven development for the first half of the year. Then, 1.5 PV (pore volume) of water is injected. After the water flooding process, 4.5 PV of CO₂ is injected for WAG flooding. The maximum cycle duration of WAG flooding is 90 days. The maximum BHP and maximum injection rate of the injector constrain the injection rate, while the

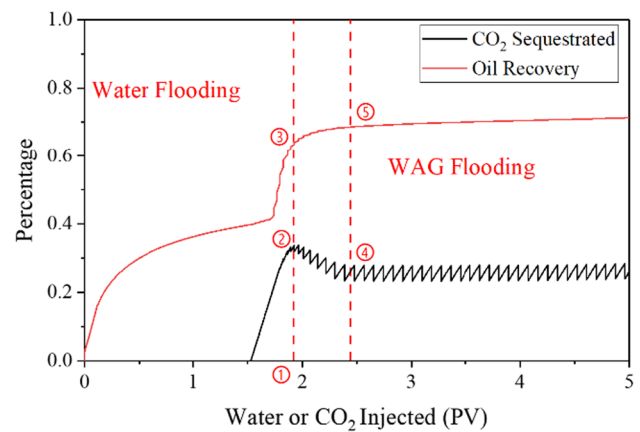


Fig. 3 Oil recovery factor and CO₂ sequestered with water or gas injected. The percentage of CO₂ sequestered means the total amount of CO₂ sequestered divided by the total formation volume

minimum BHP and maximum production rate constrain the production rate. In the base case, the maximum injection and production rates are never achieved during the simulation, and all wells are constrained by the maximum or minimum BHP. The well configuration information is presented in Table 3.

The oil recovery factor and CO₂ sequestered with water or gas injected are shown in Fig. 3. The ultimate oil recovery factor in the base case is 72.7% after WAG flooding. However, the oil recovery factor nearly stabilizes after injecting 1 PV CO₂, and this value is 68.3%. Concerning the amount of CO₂ sequestered, it increases first and then decreases after injecting 0.4 PV CO₂. The maximum amount of CO₂ sequestered is 31.9%. After injecting 1 PV CO₂, the amount of CO₂ sequestered stabilizes.

In order to compare the performance, cases of water flooding and continuous CO₂ flooding utilizing the same data set were conducted. The findings, presented in Fig. 4, illustrate the ultimate oil recovery factors of water flooding, continuous CO₂ flooding, and CO₂ WAG flooding as 41.17%, 71.53%, and 67.51%, respectively. The substantial increase in ultimate oil recovery by 26% in CO₂ WAG flooding and 30% in continuous CO₂ flooding can be attributed to the improved displacement efficiency resulting from the miscible flooding between CO₂ and crude oil. Furthermore, consistent with prior investigations (Ren and Duncan 2019b), continuous CO₂ flooding exhibits superior production performance compared to CO₂ WAG flooding, owing to the

Table 3 Well configuration information

Parameter (injector)	Value	Parameter (producer)	Value
Maximum BHP (MPa)	21.6	Minimum BHP (MPa)	7
Maximum water rate (m ³ /d)	1600	Maximum liquid rate (m ³ /d)	400
Maximum gas rate (m ³ /d)	1×10 ⁶		

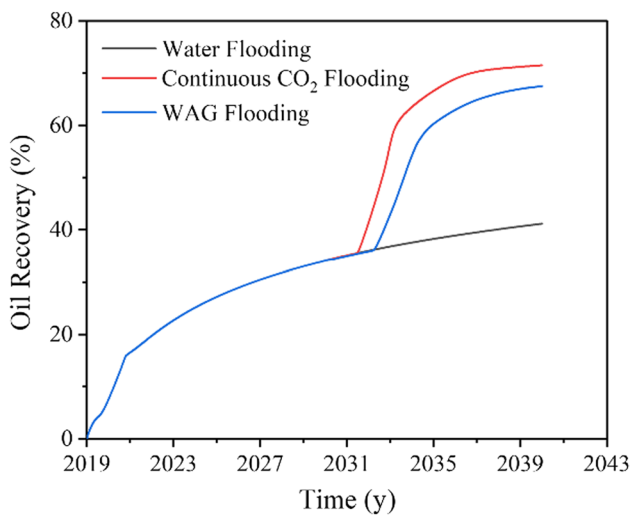


Fig. 4 Comparison of oil recovery among water flooding, continuous CO₂ flooding and WAG flooding cases

injection of a greater volume of CO₂ within the same time frame, resulting in higher sweep efficiency and displacement efficiency. However, continuous CO₂ flooding entails a cumulative injected gas volume of 6.9×10^7 m³ and a sequestered CO₂ to injected CO₂ ratio of 0.19. Conversely, CO₂ WAG flooding involves a cumulative injected gas volume of 2.8×10^7 m³ and a sequestered CO₂ to injected CO₂ ratio of 0.25. As a result, CO₂ WAG flooding offers lower injection costs and higher CO₂ sequestration efficiency, making it an attractive option in residual oil zones. The aforementioned results are derived from simulations conducted on homogeneous formations utilizing a five-spot pattern. However, the performances of continuous CO₂ flooding and CO₂ WAG flooding may vary under different conditions. For instance, in reservoirs exhibiting a rhythmic formation, WAG flooding does not present any notable advantage over water flooding

in reverse rhythmic reservoirs. Conversely, compound reverse rhythmic reservoirs could experience the greatest economic benefits from WAG flooding, as highlighted by Song et al. (2014). Furthermore, when production and injection wells are arranged in a linear drive pattern, CO₂ WAG flooding demonstrates higher oil recovery compared to continuous CO₂ flooding. The enhanced recovery achieved through WAG injection can be attributed to a more stable advancing front, resulting in improved volumetric sweep, as discussed by Namani and Kleppe (2011).

3.2 Effects of reservoir porosity

For the sensitivity analysis below, the model is carried out with the same data set and production schedule as the base case except that 1 PV CO₂ is injected rather than 4.5 PV because both oil recovery and CO₂ sequestration stabilize after injecting 1PV CO₂. Five points shown in Fig. 3 are used to help analyze the coupled CO₂-EOR and storage, where 1 refers to the amount of gas injected at the highest point of CO₂ sequestration, 2 refers to the highest amount of CO₂ sequestration, 3 refers to the oil recovery at the highest point of CO₂ sequestration, 4 refers to the amount of CO₂ sequestration after injecting 1PV CO₂, 5 refers to the ultimate oil recovery after injecting 1PV CO₂. The related parameter ranges are determined by screening criteria suitable for CO₂ flooding and storage (He et al. 2020; Khan et al. 2016; Qin et al. 2015; Shaw and Bachu 2002; Zhang et al. 2019).

Six cases with the porosity changing from 0.08 to 0.24 are designed to study the impact of reservoir porosity on coupled CO₂-EOR and storage. It is worth mentioning that the porosity does not have much influence on all five parameters when it is higher than 0.12, as shown in Fig. 5. In comparison, the coupled CO₂-EOR and storage performance gets better with the decrease in porosity

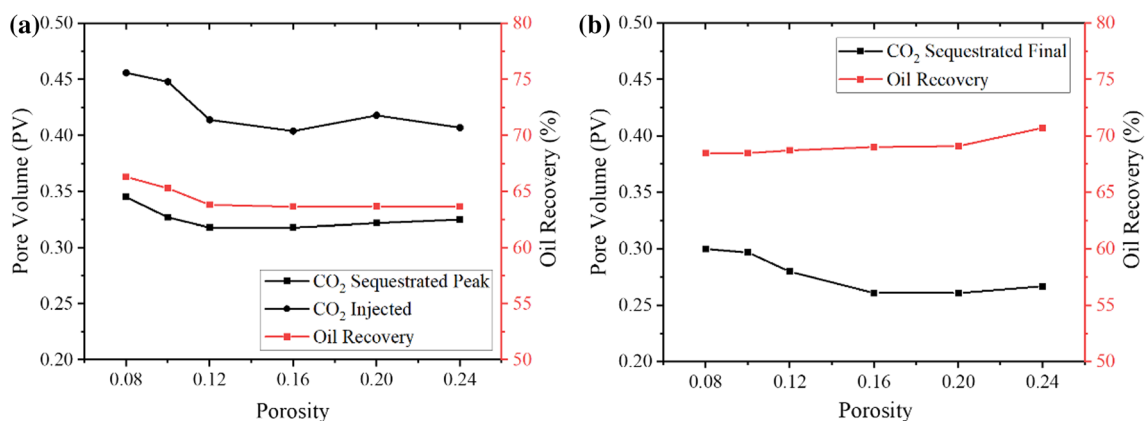


Fig. 5 Effects of reservoir porosity. **a** The highest CO₂ sequestered and its corresponding CO₂ injected and oil recovery **b** CO₂ sequestered and oil recovery after injecting 1PV CO₂

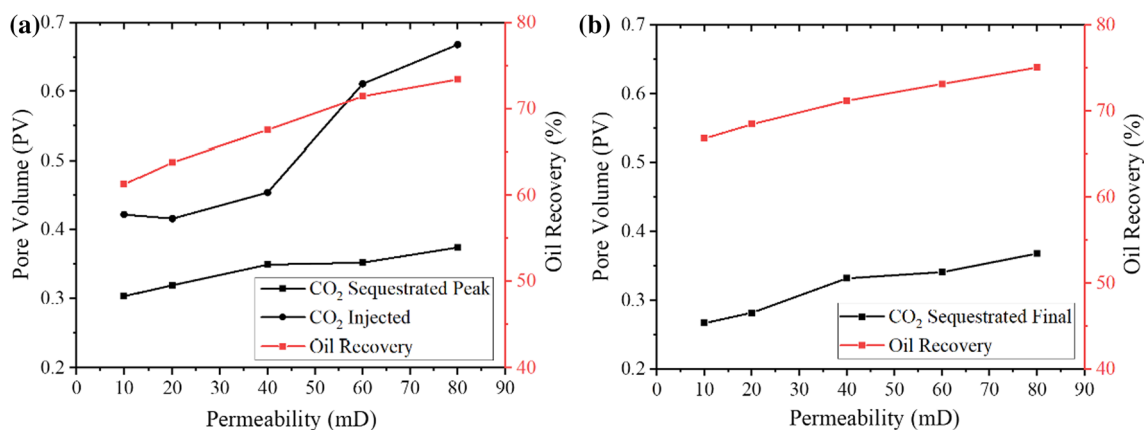


Fig. 6 Effects of reservoir permeability. **a** The highest CO₂ sequestered and its corresponding CO₂ injected and oil recovery **b** CO₂ sequestered and oil recovery after injecting 1PV CO₂

when the porosity is lower than 0.12. The reason is that the lower porosity limits the gas overriding problem, which improves the displacement efficiency of the bottom layers of the reservoir. However, this study only focuses on the relative values of oil produced and CO₂ sequestered. If the absolute values are considered, the formation with higher porosity contributes to a higher amount of CO₂ sequestered and oil produced, which is preferable for CO₂-EOR and storage projects.

3.3 Effects of reservoir permeability

Figure 6 presents the coupled CO₂-EOR and storage performance at different levels of permeability. All five parameters increase with reservoir permeability because better transmissibility improves sweep efficiency. Conversely, according to Song et al. (2014), when the permeability exceeds 400 mD, the performance of WAG flooding deteriorates due to the

exacerbation of CO₂ overriding caused by higher permeability. This reduces the sweep efficiency at the reservoir's bottom. Moreover, the rapid decline in reservoir pressure below the MMP caused by increased gas production diminishes the extent of the ultimate miscible CO₂ flooding area, jeopardizing displacement efficiency. These conclusions are predicated on analyses conducted in homogeneous reservoirs. However, for heterogeneous reservoirs, Ren and Duncan (2019b) observed that increased homogeneity in the permeability field leads to higher oil recovery and CO₂ sequestration. The presence of reservoir heterogeneity tends to induce premature CO₂ breakthrough and reduce sweep efficiency. Furthermore, Song et al. (2014) demonstrated that as the ratio of vertical to horizontal permeability increases, the efficiency of WAG flooding diminishes. This is attributable to an elevation in gas saturation within the top layer due to decreased permeability variation coefficient, subsequently accentuating the CO₂ overriding.

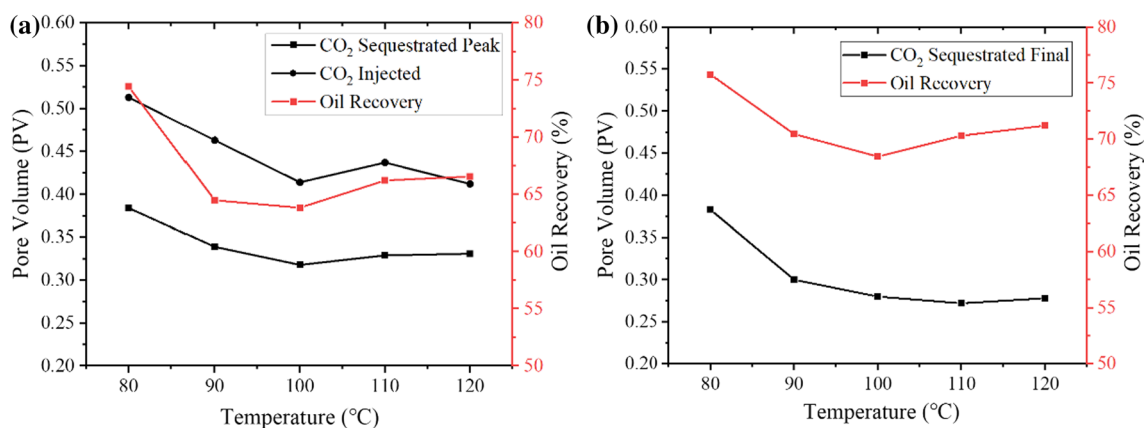


Fig. 7 Effects of reservoir temperature. **a** The highest CO₂ sequestered and its corresponding CO₂ injected and oil recovery **b** CO₂ sequestered and oil recovery after injecting 1PV CO₂

3.4 Effects of reservoir temperature

To investigate the effect of reservoir temperature, the reservoir temperature is changed from 80 to 120 °C. The results are shown in Fig. 7. When the temperature remains below 100 °C, there is a decrease observed in all five parameters with an increase in temperature, mainly because the oil has a relatively higher viscosity at lower temperatures, which makes the mobility ratio lower. The lower mobility ratio delays gas breakthrough time and improves the effect of miscible flooding. As a result, oil recovery and CO₂ sequestration increase. In contrast, When the temperature exceeds 100 °C, an increase in temperature leads to a corresponding increase in all five parameters. This is because the increase in reservoir temperature reduces oil viscosity, making the crude oil move easier toward the production well. The increased oil transmissibility improves sweep efficiency during both water flooding and WAG flooding. The findings of Perera et al. (2016) support the observed

trends, explaining that the decline in oil production as temperature rises can be attributed to CO₂ vaporization from the oil phase, which limits contact with the oil. Conversely, the substantial increase in oil production at higher temperatures is ascribed to the prevailing impact of kinetic energy increment, accompanied by a corresponding rise in CO₂ mobility. This effect outweighs the influence of CO₂ vaporization in high-temperature conditions.

3.5 Effects of diffusion coefficient of oil and gas

The diffusion coefficients of seven pseudo-components in oil and gas phases are set from 0.01 to 0.03 cm²/s and from 10⁻⁶ to 2.4 × 10⁻⁶ cm²/s, respectively. Figure 8 compares the results of different gas diffusion coefficients and shows that all other four parameters decrease with the increase in gas diffusion coefficient except for the amount of gas injected at the highest point of CO₂ sequestration. The results indicate that gas diffusion harms the coupled CO₂-EOR and storage.

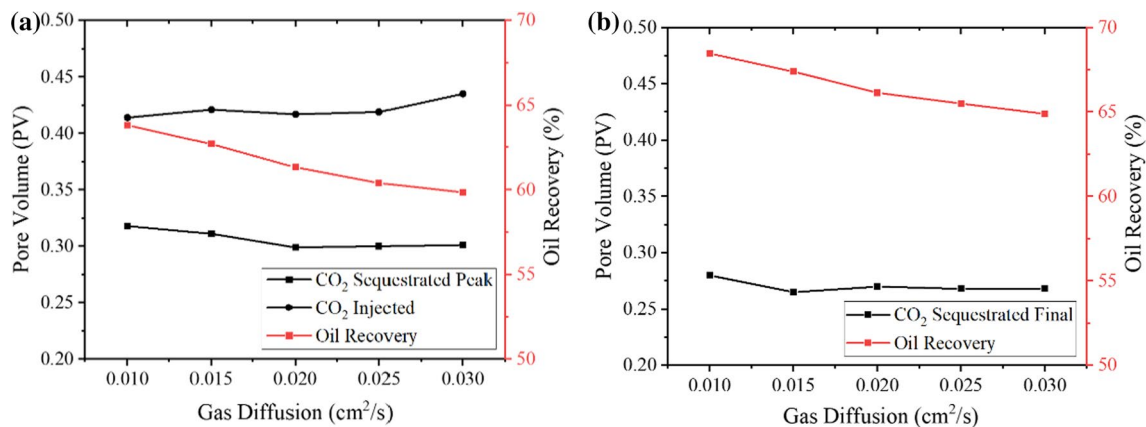


Fig. 8 Effects of gas diffusion coefficient. **a** The highest CO₂ sequestered and its corresponding CO₂ injected and oil recovery **b** CO₂ sequestered and oil recovery after injecting 1PV CO₂

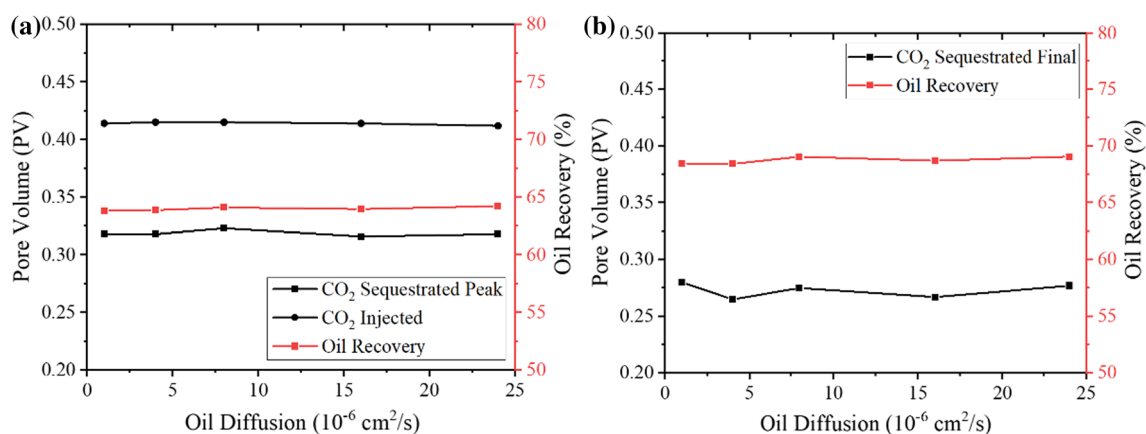


Fig. 9 Effects of oil diffusion coefficient. **a** The highest CO₂ sequestered and its corresponding CO₂ injected and oil recovery **b** CO₂ sequestered and oil recovery after injecting 1PV CO₂

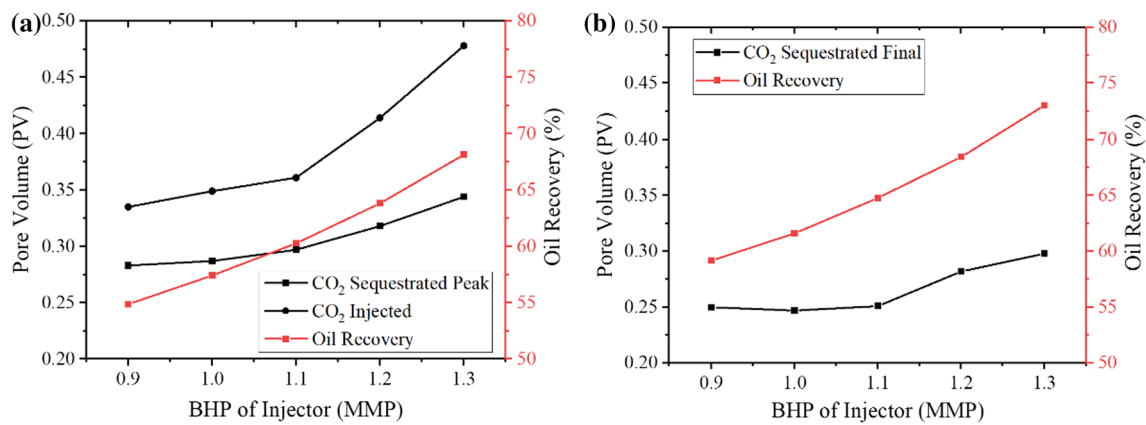


Fig. 10 Effects of BHP of injection well. **a** The highest CO₂ sequestered and its corresponding CO₂ injected and oil recovery **b** CO₂ sequestered and oil recovery after injecting 1PV CO₂

This is because gas diffusion improves gas transmissibility, worsening the gas overriding problem and leading to a lower displacement efficiency. The ultimate oil recovery and CO₂ sequestered decrease by 3.6% and 1.2%, respectively, with the change in gas diffusion coefficient from 0.01 to 0.03 cm²/s. On the contrary, the diffusion in the oil phase has a limited impact on the coupled CO₂-EOR and storage, as described in Fig. 9. This is because the oil diffusion coefficient is four orders of magnitude lower than the gas diffusion coefficient.

3.6 Effects of BHP of injection well and production well

The BHPs of the injection and production wells play an important role in WAG flooding as they determine the feasibility of maintaining the MMP. In this study, the BHP of the injection well is varied within the range of 0.9 MMP to 1.4 MMP, as depicted in Fig. 10. Notably, a clear increment is

observed for all five data points as the BHP of the injection well increases, particularly when it exceeds 1.1 MMP, aligning with the findings of a previous study (Yan and Stenby 2009). This phenomenon can be attributed to the attainment and sustainable maintenance of the desired miscible flooding state over a more extensive area, resulting in enhanced final displacement efficiency. Moreover, this improvement is attributed to the augmented injection rate facilitated by the enhanced BHP (Ren and Duncan 2019b). The higher injection rate intensifies the viscous force and reduces the time required for gravity force to segregate the fluids, as highlighted by Namani and Kleppe (2011).

The BHP of the production well is selected from 3000 to 11,000 kPa to investigate its influence on the coupled CO₂-EOR and storage, as shown in Fig. 11. The coupled CO₂-EOR and storage performance does not change a lot, except that the BHP of the production well increases from 5000 to 7000 kPa. This is because if the production pressure differential is too high, the displacement pressure cannot be

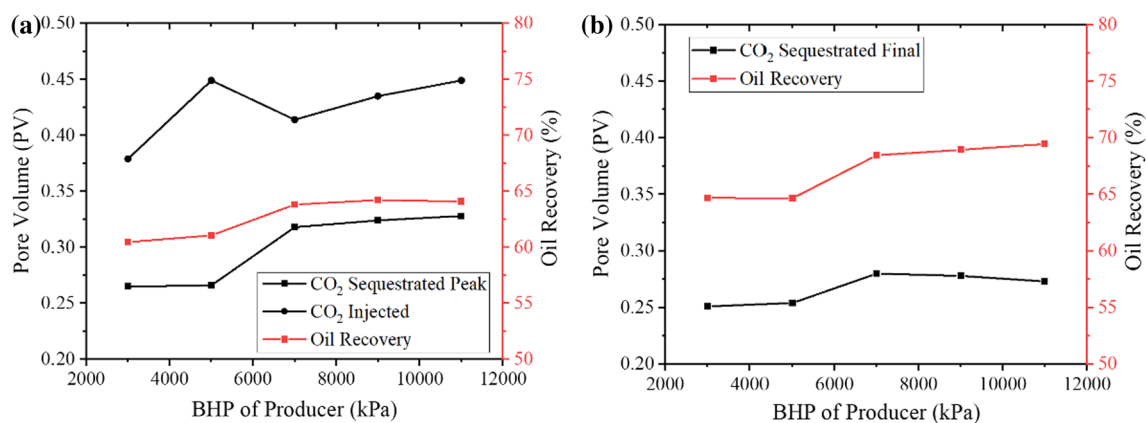


Fig. 11 Effects of BHP of production well. **a** The highest CO₂ sequestered and its corresponding CO₂ injected and oil recovery **b** CO₂ sequestered and oil recovery after injecting 1PV CO₂

Table 4 Tapered WAG design

WAG ratio	Duration (years)
0.5:1	3
1:1	3
2:1	3
4:1	To end

maintained above the MMP, jeopardizing the displacement efficiency and the performance of the coupled CO₂-EOR and storage.

3.7 Effects of WAG ratio

The cases of different WAG ratios and tapered WAG are carried out to investigate their effects on coupled CO₂-EOR and storage. Five WAG ratio patterns are under investigation. Pattern 1 refers to the WAG ratio of 0.5:1, which means 45 days of water injection followed by 90 days of CO₂ injection. Patterns 2, 3, and 4 refer to the WAG ratios of 1:1, 2:1, and 4:1, respectively. The meanings are the same as in pattern 1. Pattern 5 refers to the tapered WAG ratio shown in Table 4. As shown in Fig. 12, the coupled CO₂-EOR and storage performance worsens as the WAG ratio increases, which is supported by Kohata et al. (2017). The reason is that the hindrance of oil and CO₂ contact resulting from a large volume of injected water negatively impacts the efficiency of miscible flooding. Moreover, tapered WAG flooding demonstrates favorable performance in terms of oil enhancement. However, when the objective is CO₂ sequestration, with a focus on injecting the maximum amount of CO₂ and achieving the desired oil recovery, the overall performance of Pattern 1 surpasses that of tapered WAG

flooding. Additionally, the optimal WAG ratio for projects in ROZs is influenced by whether the zone is a virgin ROZ or a man-made waterflooding (MMWF) zone, as highlighted by Ren and Duncan (2021). It is speculated that the prevalent high water saturation in virgin ROZs contributes to consistently smaller favorable WAG ratios in virgin ROZs compared to those in zones following MMWF. Notably, the performance of coupled CO₂-EOR and storage is contingent not only upon the WAG ratio but also on the half-cycle time. Namani and Kleppe (2011) underscored that cases with shorter gas injection times exhibit reduced oil recovery, while a decrease in water injection time has minimal impact on the oil recovery factor. Therefore, when designing WAG flooding, careful consideration must be given to the WAG ratio, cycle time, and half-cycle duration.

3.8 Effects of PV of water injected

The efficacy of coupled CO₂-EOR and storage is affected by the volume of water injected during the water flooding. To investigate the impact of water injection on the coupled process, simulations are conducted with varying volumes of injected water: 1 PV, 2 PV, 4 PV, and 6 PV. Figure 13 illustrates that all five parameters exhibit an increasing trend with the progressive injection of water. This phenomenon can be attributed to the enhancement of sweep efficiency and displacement efficiency associated with higher volumes of water injection. However, the absence of miscible flooding during water flooding limits the significant improvement in displacement efficiency, resulting in a modest increase of only 2% and 3.5% in ultimate oil recovery and CO₂ sequestration, respectively.

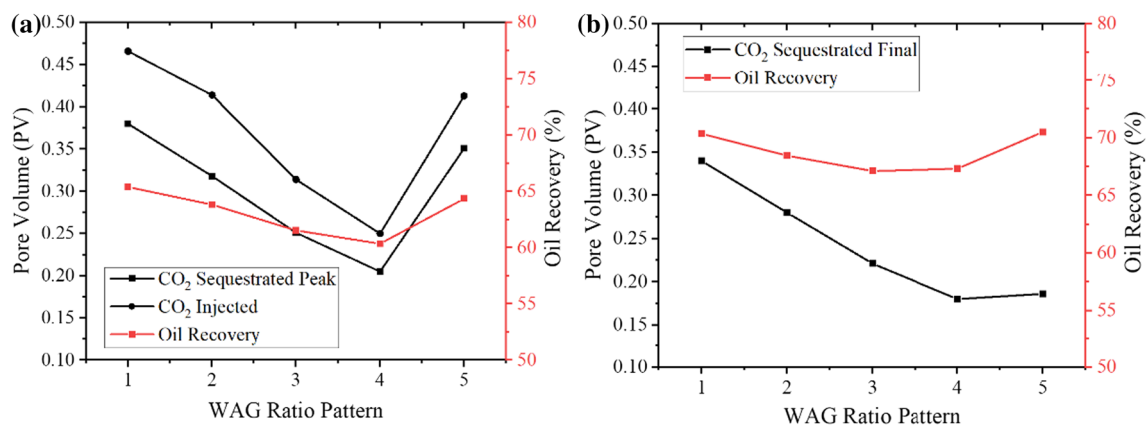


Fig. 12 Effects of the WAG ratio. **a** The highest CO₂ sequestered and its corresponding CO₂ injected and oil recovery **b** CO₂ sequestered and oil recovery after injecting 1PV CO₂

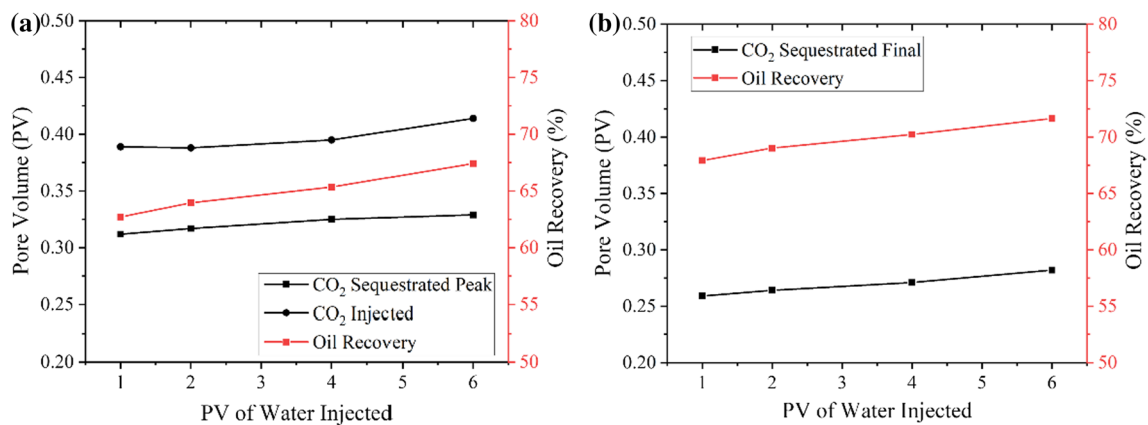


Fig. 13 Effects of the PV of water injected. **a** The highest CO₂ sequestered and its corresponding CO₂ injected and oil recovery **b** CO₂ sequestered and oil recovery after injecting 1PV CO₂

4 Conclusions

This paper conducted a numerical study on the coupled CO₂-EOR and storage performance in ROZs. The sensitivity analysis was designed to investigate the optimal parameters with molecular diffusion. The conclusions are as follows.

- (1) The reservoir porosity does not greatly influence the relative values of oil produced and CO₂ sequestered if it is larger than 0.12. In comparison, the coupled CO₂-EOR and storage performance gets better with the decrease in porosity when the porosity is lower than 0.12.
- (2) The coupled CO₂-EOR and storage performance improves with the increased reservoir permeability because of the better sweep efficiency achieved. However, the MMP might not be maintained long if the permeability is too high.
- (3) When the temperature is around 100 °C, the coupled CO₂-EOR and storage exhibit their most unfavorable performance, which results from the combination of gas breakthrough and a change in gas transmissibility.
- (4) The increased gas diffusion coefficient lowers the amount of oil produced and CO₂ sequestered due to the enhanced gas breakthrough. In contrast, the effect of oil diffusion is small because the oil diffusion coefficient is four orders of magnitude lower than the gas diffusion coefficient.
- (5) The BHP of the injection well is supposed to be higher than 1.2 MMP during the WAG flooding to achieve ideal miscible flooding. The BHP of the production well should not be too low. If the production pressure differential exceeds a certain limit, the displacement pressure cannot be maintained above the MMP.

- (6) By increasing the WAG ratio from 0.5 to 4, the amounts of CO₂ sequestration and oil recovery decrease. Besides, tapered WAG flooding is promising when the goal is ultimate oil recovery. However, for CO₂ sequestration, whose goal is to inject as much CO₂ as possible and achieve the desired oil recovery, the overall performance of 0.5 WAG ratio is the best.

Acknowledgements This work was supported by the National Natural Science Foundation of China (52034010)

Authors contributions BL: Conceptualization, methodology, software, investigation, writing-original draft. JY: validation, writing-review & editing, supervision, project administration, funding acquisition. TS: software, resources.

Funding This work was supported by the National Natural Science Foundation of China (52034010).

Availability of data and materials Data available on request from the authors.

Declarations

Competing interests The authors declare that they have no conflict of interest.

Open Access This article is licensed under a Creative Commons Attribution 4.0 International License, which permits use, sharing, adaptation, distribution and reproduction in any medium or format, as long as you give appropriate credit to the original author(s) and the source, provide a link to the Creative Commons licence, and indicate if changes were made. The images or other third party material in this article are included in the article's Creative Commons licence, unless indicated otherwise in a credit line to the material. If material is not included in the article's Creative Commons licence and your intended use is not permitted by statutory regulation or exceeds the permitted use, you will need to obtain permission directly from the copyright holder. To view a copy of this licence, visit <http://creativecommons.org/licenses/by/4.0/>.

References

- Agarwal R, Li YK, Nghiem L (1987) A regression technique with dynamic-parameter selection or phase behavior matching. In: SPE california regional meeting
- Al Eidan AA, Bachu S, Melzer LS, Lars EI, Ackiewicz M (2015) Technical challenges in the conversion of CO₂-EOR projects to CO₂ storage projects. In: SPE asia pacific enhanced oil recovery conference
- Brock WR, Bryan LA (1989) Summary results of CO₂ EOR field tests. In: Low permeability reservoirs symposium
- Ettehadtavakkol A, Lake LW, Bryant SL (2014) CO₂-EOR and storage design optimization. *Int J Greenhouse Gas Control* 25:79–92. <https://doi.org/10.1016/j.ijggc.2014.04.006>
- Farajzadeh R, Andrianov A, Zitha PLJ (2010) Investigation of immiscible and miscible foam for enhancing oil recovery. *Ind Eng Chem Res* 49:1910–1919
- Ghaderi SM, Clarkson CR, Chen S (2012) Optimization of WAG process for coupled CO₂ EOR-storage in tight oil formations: an experimental design approach. In: SPE Canadian unconventional resources conference
- Gong Y, Gu Y (2015) Miscible CO₂ simultaneous water-and-gas (CO₂-SWAG) injection in the bakken formation. *Energy Fuels* 29(9):5655–5665. <https://doi.org/10.1021/acs.energyfuels.5b01182>
- He Y, Zhao S, Bingyu JI, Liao H, Zhou Y, Amp PE, SINOPEC (2020) Screening method and potential evaluation for EOR by CO₂ flooding in sandstone reservoirs. In: Petroleum geology and recovery efficiency.
- Jiang K, Ashworth P, Zhang S, Liang X, Sun Y, Angus D (2020) China's carbon capture, utilization and storage (CCUS) policy: a critical review. *Renewable Sustainable Energy Rev* 119:109601. <https://doi.org/10.1016/j.rser.2019.109601>
- Karimaie H, Nazarian B, Aurdal T, Nøkleby PH, Hansen O (2017) Simulation study of CO₂ EOR and storage potential in a north sea reservoir. *Energy Procedia* 114:7018–7032. <https://doi.org/10.1016/j.egypro.2017.03.1843>
- Khan MY, Kohata A, Patel H, Syed FI, Al Sowaidi AK (2016) Water alternating gas WAG optimization using tapered WAG technique for a giant offshore middle east oil field. In: Abu Dhabi international petroleum exhibition & conference
- Kohata A, Willingham T, Yunus Khan M, Al Sowaidi A (2017) Extensive miscible water alternating gas WAG simulation study for a giant offshore oil field. In: Abu Dhabi international petroleum exhibition & conference
- Koperna GJ, Melzer LS, Kuuskraa VA (2006) Recovery of oil resources from the residual and transitional oil zones of the permian basin. In: SPE annual technical conference and exhibition
- Liu S, Ji C, Wang C, Chen J, Jin Y, Zou Z, Zou J (2018) Climatic role of terrestrial ecosystem under elevated CO₂: a bottom-up greenhouse gases budget. *Ecol Lett* 21(7):1108–1118. <https://doi.org/10.1111/ele.13078>
- Namani M, Kleppe J (2011) Investigation of the effect of some parameters in miscible WAG process using black-oil and compositional simulators. In: SPE enhanced oil recovery conference
- Peng D-Y, Robinson DB (1976) A new two-constant equation of state. *Ind Eng Chem Fundam* 15(1):59–64. <https://doi.org/10.1021/i160057a011>
- Perera MSA, Gamage RP, Rathnaweera TD, Ranathunga AS, Koay A, Choi X (2016) A review of CO₂-enhanced oil recovery with a simulated sensitivity analysis. *Energies* 9(7):481
- Qin J, Han H, Liu X (2015) Application and enlightenment of carbon dioxide flooding in the United States of America. *Petrol Explor Dev* 42(2):232–240. [https://doi.org/10.1016/S1876-3804\(15\)30010-0](https://doi.org/10.1016/S1876-3804(15)30010-0)
- Ren B, Duncan I (2019) Modeling oil saturation evolution in residual oil zones: implications for CO₂ EOR and sequestration. *J Petrol Sci Eng* 177:528–539. <https://doi.org/10.1016/j.petrol.2019.02.072>
- Ren B, Duncan I (2019) Reservoir simulation of carbon storage associated with CO₂ EOR in residual oil zones San Andres formation of West Texas, Permian Basin, USA. *Energy* 167:391–401. <https://doi.org/10.1016/j.energy.2018.11.007>
- Ren B, Duncan IJ (2021) Maximizing oil production from water alternating gas (CO₂) injection into residual oil zones: the impact of oil saturation and heterogeneity. *Energy* 222:119915. <https://doi.org/10.1016/j.energy.2021.119915>
- Rui Z, Peng F, Ling K, Chang H, Chen G, Zhou X (2017) Investigation into the performance of oil and gas projects. *J Natl Gas Sci Eng* 38:12–20. <https://doi.org/10.1016/j.jngse.2016.11.049>
- Shaw J, Bachu S (2002) Screening, evaluation, and ranking of oil reservoirs suitable for CO₂-flood EOR and carbon dioxide sequestration. *J Can Petrol Technol*. <https://doi.org/10.2118/02-09-05>
- Song Z, Li Z, Wei M, Lai F, Bai B (2014) Sensitivity analysis of water-alternating-CO₂ flooding for enhanced oil recovery in high water cut oil reservoirs. *Comput Fluids* 99:93–103. <https://doi.org/10.1016/j.compfluid.2014.03.022>
- Stone (1970) Probability model for estimating three-phase relative permeability. *J Petrol Technol* 22(02):214–218
- Yan W, Stenby EH (2009). The influence of CO₂ solubility in brine on CO₂ flooding simulation. In: SPE annual technical conference and exhibition
- Zhang N, Yin M, Wei M, Bai B (2019) Identification of CO₂ sequestration opportunities: CO₂ miscible flooding guidelines. *Fuel* 241:459–467. <https://doi.org/10.1016/j.fuel.2018.12.072>

Publisher's Note Springer Nature remains neutral with regard to jurisdictional claims in published maps and institutional affiliations.